

Clinical Performance of 2 Dedicated PET Scanners for Breast Imaging: Initial Evaluation

Mami Iima¹, Yuji Nakamoto¹, Shotaro Kanao¹, Tomoharu Sugie², Takayuki Ueno², Mayumi Kawada³, Yoshiki Mikami⁴, Masakazu Toi², and Kaori Togashi¹

¹Department of Diagnostic Imaging and Nuclear Medicine, Kyoto University Graduate School of Medicine, Kyoto, Japan;

²Department of Breast Surgery, Kyoto University Graduate School of Medicine, Kyoto, Japan; ³Department of Gastroenterology and Hepatology, Kyoto University Graduate School of Medicine, Kyoto, Japan; and ⁴Department of Diagnostic Pathology, Kyoto University Graduate School of Medicine, Kyoto, Japan

The purpose of this study was to investigate the diagnostic performance of 2 newly developed dedicated breast PET scanners in patients with known or suspected breast cancer.

Methods: Two types of scanner were evaluated, an O-shaped scanner and a C-shaped scanner. The O scanner was designed for imaging patients who were prone, and the C scanner was designed for those patients positioned leaning forward. Sixty-nine women with known or suspected breast carcinoma (80 lesions: 72 invasive carcinomas, 4 noninvasive carcinomas [ductal carcinoma in situ, or DCIS], 1 case of adenomatous ductal hyperplasia, and 3 benign lesions) were enrolled in this study. All patients underwent a conventional whole-body PET/CT scan, followed by breast scanning using both dedicated devices. The diagnostic performance of each scanner was assessed.

Results: The maximal diameter of invasive tumors ranged from 4 to 112 mm, with an average of 26 mm. With the O scanner, 62 of 76 malignant lesions (including 3 DCIS) were detected, 5 lesions were not detected, and the remaining 9 lesions were outside the field of view. With the C scanner, 63 of 76 malignant lesions (including 2 DCIS) were detected, 7 lesions were not detected, and the remaining 6 lesions were outside the field of view. The lesion-based sensitivities of the O and C scanners were 82% (62/76) and 83% (63/76), respectively; sensitivities excluding lesions outside the field of view were 93% (62/67) and 90% (63/70), respectively. The sensitivity of conventional PET/CT was 92% (70/76). All lesions outside the field of view were close to the chest wall. The breast-based specificities of the O, C, and conventional scanners were 98% (48/49), 98% (56/57), and 100% (70/70), respectively.

Conclusion: Our preliminary study indicates that both dedicated breast PET scanners are clinically feasible and yield reasonably high sensitivity. More detailed information was obtained with these scanners than with the conventional scanner.

Key Words: breast cancer; dedicated; ¹⁸F-FDG; positron emission mammography (PEM); PET/CT

J Nucl Med 2012; 53:1534–1542

DOI: 10.2967/jnumed.111.100958

Breast cancer is one of the most common cancers worldwide, with approximately 39,520 women in the United States estimated to have died from this disease in 2011 (1). Screening mammography has been established as an important factor in the recent decline of breast cancer mortality (2). The PET technique using the radiolabeled glucose analog ¹⁸F-FDG has successfully been introduced in the diagnosis of breast cancer, and several groups have demonstrated a high diagnostic ability for breast cancer using ¹⁸F-FDG PET (3–5), even higher than with ultrasound or mammography (6). However, there are some limitations in the detection of small breast cancers, partly because of the insufficient spatial resolution of the modality (7). Nevertheless, it is important to detect breast cancer at an early stage in order to obtain a high degree of curability through the use of less invasive procedures.

To overcome such limitations, dedicated PET scanners for breast imaging have been developed, and initial reports have described the potential clinical value of the higher spatial resolution and sensitivity that is achievable with these devices (8–10). Bowen et al. (11) classified dedicated PET scanners for breast imaging into 2 groups. The first group comprises positron emission mammography (PEM) systems, which use limited-angle tomography with 2 planar or curved detectors (12–14); the second scanner group acquires fully tomographic images of the breast (11,15). For the PEM system, a multicenter trial of 94 patients showed improved sensitivity for the detection of small cancers, including ductal carcinoma in situ (DCIS) (16), and PEM was considered comparable to MRI as a presurgical breast imaging modality (17,18). However, the feasibility and diagnostic performance of the full tomography-based dedicated PET system for a relatively large number of

Received Dec. 5, 2011; revision accepted May 21, 2012.

For correspondence contact: Yuji Nakamoto, Department of Diagnostic Imaging and Nuclear Medicine, Kyoto University Graduate School of Medicine, 54 Shogoin-Kawahara-cho, Sakyo-ku, Kyoto, 606-8507 Japan.

E-mail: ynakamo1@kuhp.kyoto-u.ac.jp

Published online Aug. 29, 2012.

COPYRIGHT © 2012 by the Society of Nuclear Medicine and Molecular Imaging, Inc.

patients has not yet been demonstrated. Because the clinical role of these dedicated PET scanners has not been established, we need to keep investigating the advantage of these scanners in the clinical setting.

Novel dedicated PET scanners that detect breast cancer with high spatial resolution and sensitivity have been developed and introduced at our institute. Two types of scanners have been developed: an O-shaped scanner and a C-shaped scanner. The O-shaped device was designed for scanning patients who were positioned prone, yielding images that are easy to merge with MR images. The C-shaped scanner was designed to image patients leaning forward, whereby data can be acquired more comfortably for the patient.

The purpose of this study was to evaluate the diagnostic performance of the 2 dedicated PET scanners, comparing their performance with a conventional PET/CT scanner and breast MRI scanner, in patients who were known to have or suspected of having breast cancer.

MATERIALS AND METHODS

Patients and Lesion Characteristics

Consecutive women ($n = 107$) who were known to have or suspected of having breast carcinoma—on the basis of the results of physical examination, mammography, ultrasound, or MRI—underwent conventional whole-body PET/CT, followed by breast scanning using a dedicated PET device, from November 2009 to January 2011. Thirty-eight patients were excluded, including those who had received neoadjuvant chemotherapy or endocrine therapy before PET ($n = 24$); those who were not scanned by either dedicated scanner, in order to accommodate patients' requests ($n = 12$); and those for whom MRI was not performed because of contraindications ($n = 2$). Thus, 69 patients were analyzed in this study. Our institutional review board approved the study, and written informed consent was obtained from all patients.

Conventional PET/CT and Dedicated PET

Patients fasted for at least 4 h before the examination, and their plasma glucose level was checked just before the administration of ^{18}F -FDG (~ 3.7 MBq/kg of weight). There were no patients with a plasma glucose level greater than 200 mg/dL in this population. About 1 h later, conventional PET/CT was performed first, using a combined PET/CT scanner (Discovery ST Elite; GE Healthcare) for 2–3 min/bed position, followed by breast scanning using the

O and C scanners for 5 min for each breast. The 5-min scan time in both scanners was determined by preliminary evaluations (19) demonstrating that image quality was almost equivalent between images acquired by a 4- to 6-min scan and those acquired by a 10-min scan.

Both dedicated scanners have depth-of-interaction detectors consisting of a 4-layer $32 \times 32 \text{ Lu}_{1.8}\text{Gd}_{0.2}\text{SiO}_5$ (Hitachi Chemical) crystal array, a light guide, a 64-channel flat-panel-type photo-multiplier tube (H8500; Hamamatsu Photonics), and a $1.44 \times 1.44 \times 4.5$ mm crystal element. The total detector thickness is 18 mm, and the pitch is 1.53 mm. More detailed technical information can be found elsewhere (20). The O scanner has a full-ring detector, comprising 36 detector modules arranged in a 3-ring configuration with a diameter of 195 mm and an axial extent of 155.5 mm. The detector of the C scanner has an open end in which the patient's arm can be placed (Supplemental Fig. 1 [supplemental materials are available online only at <http://jnm.snmjournals.org>]). The detector ring consists of 24 detector modules arranged in a 2-ring configuration, with a diameter of 228 mm and an axial extent of 105 mm. The transaxial effective fields of view of the O and C scanners were 180 and 179 mm in diameter, respectively. All acquisition data were reconstructed by 1 iteration and 128 subsets of a 3-dimensional list-mode dynamic row-action maximum likelihood algorithm with a point spread function model (21). The energy and time resolution of the detector were 16.9% and 1.2 ns, respectively. The sensitivity of the O and C scanners measured with a ^{22}Na point source was 16.3% and 6.9%, respectively. The spatial resolution of these scanners measured with an ^{18}F point source was estimated to be less than 2 mm. Testing with a phantom that had rod sources of various diameters placed at a 20-mm radial offset from the center showed that both scanners could visualize a 2-mm hot rod in the air and a 3-mm hot rod in the uniform background (activity concentration ratio of ^{18}F , 4:1) (20). The order of scanning with the O and C devices was determined randomly to avoid bias, and the mean duration between ^{18}F -FDG injection and the start of scanning was 104.7 min (range, 75–129 min) for the O device and 105.6 min (range, 69–145 min) for the C device. No attenuation correction was performed for dedicated PET. The specifications of these scanners are summarized in Table 1. Also, the appearance of the scanners and schema of detectors and the field of view are demonstrated in Figure 1.

MRI

Breast MRI was performed using a 1.5-T system (Avanto; Siemens Medical Solutions) equipped with a dedicated 4-channel

TABLE 1
Specifications of O and C PET

Specification	O PET	C PET
Detector ring configuration	Full ring	C-shaped
No. of detector modules	36 (12 modules \times 3 rings)	24 (12 modules \times 2 rings)
Axial field of view (mm)	155.5	105
Transaxial field of view (mm)	183	216
Energy resolution (%)	16.90	16.90
Time resolution (ns)	1.2	1.2
Spatial resolution (mm)	<2	<2
Maximum true counting rate (kcps)	763	300
Sensitivity (%)	16.30	6.90
Scatter fraction (%)	38	31

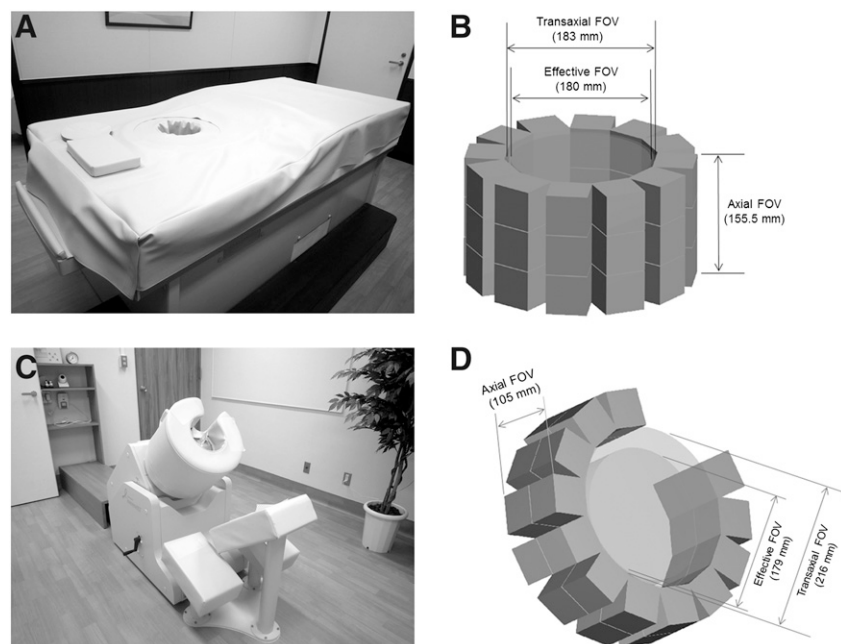


FIGURE 1. Appearance and schema of field of view of O scanner (A and B) and C scanner (C and D). O scanner has full-ring detectors with smaller gantry. Because patients are scanned while prone, registration of PET images to MR images is easy and reliable. On the other hand, a segment of detectors is missing in C scanner, providing larger field of view for breast imaging. Data acquisition can be performed with patient in forward-leaning posture. It is not necessary to stabilize the breast when using these scanners. FOV = field of view.

breast array coil. The following images were obtained after localizers were acquired: bilateral fat-suppressed T2-weighted images (repetition time/echo time, 5,500/83 ms; flip angle, 140°; field of view, 330 mm; matrix, 448 × 336; slice thickness, 3.0 mm; reconstructed resolution, 0.7 × 1.0 × 3.0 mm; and acquisition time, 90 s); non-fat-suppressed T1-weighted images; and fat-suppressed T1-weighted dynamic contrast-enhanced images obtained using a 3-dimensional fat-suppressed gradient-echo sequence (repetition time/echo time, 4.0/1.4 ms; flip angle, 15°; field of view, 330 mm; matrix, 448 × 336; slice thickness, 1.5 mm; reconstructed resolution, 0.7 × 1.0 × 1.5 mm; and acquisition time, 60 s). The fat-suppressed T1-weighted dynamic contrast-enhanced images were acquired before and 3 times (0–1, 1–2, and 5–6 min) after injection of a gadolinium-based contrast agent (gadoteridol [ProHance; Eisai] or gadodiamide [Omniscan; Daiichi-Sankyo]).

Image Analysis

The ¹⁸F-FDG conventional PET/CT and dedicated PET images were visually evaluated by 2 individuals board-certified in both radiology and nuclear medicine by consensus. The PET/CT images were evaluated on an Advantage workstation (version 4.4; GE Healthcare), and the maximum standardized uptake values were calculated. The dedicated PET images were analyzed on another workstation (AquariusNet; TeraRecon), and the observers were masked to all clinical information and radiologic findings. Focal moderate to intense uptake, compared with surrounding tissue, was regarded as positive. When the uptake was high but was difficult to differentiate from noise, it was considered negative. MRI data were evaluated by 2 radiologists on a PACS workstation (Centricity PACS; GE Healthcare). Breast lesions were evaluated according to the American College of Radiology Breast Imaging Reporting and Data System (22), with all clinical and imaging information available at interpretation.

T staging and maximal diameter of all lesions were assessed on the basis of morphology seen on conventional PET/CT and on MR images, and T4 tumors were categorized according to their size, as in the study by Avril et al. (23). When multiple lesions were

observed on 1 side, 2 representative lesions (usually the largest and second largest) were analyzed to obtain a more reliable correlation between radiologic findings and pathologic results after surgery. The diagnostic performance of each modality was calculated on a patient basis, breast basis, and lesion basis using the final diagnosis.

Standard of Reference

All malignant tumors and atypical ductal hyperplasia were histopathologically confirmed after surgery. All benign lesions were diagnosed by biopsy and by lack of tumor growth on ultrasonographic or radiologic monitoring during a follow-up period of at least 18 mo (24). Furthermore, breasts with no abnormal findings were finally regarded as negative on the basis of clinical or radiologic follow-up of at least 8 mo. All pathologic results were defined according to the classification of breast tumors by the World Health Organization (25).

RESULTS

The flowchart in Figure 2 demonstrates the number of patients, breasts, and known or suspected lesions evaluated in this study. Sixty-nine patients (age range, 31–77 y; mean age, 53.5 y), 137 breasts, and 80 lesions (right, $n = 39$; left, $n = 41$) were analyzed in this investigation. Breasts without suspected lesions were not always scanned by both dedicated scanners, in order to accommodate patients' requests or because of a previous history of mastectomy, although breasts with known or suspected lesions were scanned by both scanners. Thus, 117 breasts were analyzed using the O scanner and 125 breasts using the C scanner. Of 80 lesions, 76 lesions were malignant (72 invasive carcinomas), 1 lesion was atypical ductal hyperplasia, and 3 lesions (1 fibroadenoma in 1 patient and 2 fibrocystic changes in 1 patient) were benign.

Of the 76 malignant lesions in 67 patients, 67 were invasive ductal carcinomas (15 grade I lesions, 41 grade II lesions, and 11 grade III lesions), 5 were invasive lobular carcinomas, and 4 were DCIS (noninvasive ductal carcinoma). The size of the invasive carcinomas ranged from 4 to 112 mm, with an average of 26 mm. The maximum standardized uptake value on conventional PET/CT ranged from 1.0 to 20.4, with an average of 5.8. Among the lesions, 54 lesions had been examined using a core-needle biopsy (20 lesions) or a vacuum-assisted biopsy (34 lesions) before PET. The characteristics of the lesions evaluated by the O and C scanners are summarized in Table 2. The sensitivity and specificity of each scanner on a patient, breast, and lesion basis are demonstrated in Tables 3, 4, and 5, respectively. In addition, the sensitivities of dedicated PET and conventional PET/CT according to T staging and histopathologic subtypes are given in Table 6.

O Scanner

Sixty-two of 76 malignant lesions (82%) were positive, whereas 14 lesions were not detected. Of these 14 lesions, 5 lesions could not be identified despite being within scanning range, and the remaining 9 lesions were considered outside the field of view. All missed lesions outside the scanning range were close to the chest wall. Excluding lesions outside the field of view, the lesion-based and patient-based sensitivities were 93% (62/67) and 93% (55/59), respectively. The O scanner depicted 59 of 64 invasive carcinomas (92%) and 3 of 3 DCIS (100%). There were 7 lesions that were not detected by mammography but were identified by the O scanner (mean size, 17.5 mm). The breast-based specificity was 98% (48/49). A representative case is shown in Figure 3, in which 2 lesions were identified on O, C, and MRI scanning conventional PET/CT demonstrated 1 lesion only. Figure 4 shows the case in which the appearance was different between O PET and conventional PET/CT and hematoxylin and eosin staining and immunohistochemical staining for hexokinase II activity were performed.

C Scanner

Of 76 malignant lesions, 63 lesions (83%) were depicted, and 13 lesions were negative. Among the 13 lesions, 7 lesions were not visualized, and the remaining 6 lesions were considered out of the scanning range. The overall lesion-based sensitivity was 83% (63/76). After 6 lesions outside the field of view were excluded, lesion-based sensitivity was 90% (63/70), and the patient-based sensitivity was 92% (57/62). Sixty-one of 67 invasive carcinomas (91%), and 2 of 3 DCIS (67%) were detected with this scanner. There were 6 lesions that had not been detected by mammography (mean size, 19.5 mm). The breast-based specificity was estimated to be 98% (56/57). There were no significant differences of diagnostic performance between the 2 dedicated PET scanners (McNemar test).

Conventional PET/CT and MRI

In this population, the patient-based, breast-based, and lesion-based sensitivities of conventional PET/CT were 96% (64/67), 96% (65/68), and 92% (70/76), respectively, whereas those of MRI were 100% (67/67), 100% (68/68), and 100% (76/76), respectively. PET/CT detected 66 of 72 invasive carcinomas (92%) and 4 of 4 DCIS (100%). The breast-based specificities of PET/CT and MRI were 100% (70/70) and 100% (70/70), respectively.

DISCUSSION

Since Thompson et al. first reported on the feasibility of using PEM with a 2-detector-array system by evaluating a breast phantom (26), some groups have reported that PEM has a good ability to detect small breast cancers, including DCIS (16,27). In the new dedicated PET systems described here, images of the breast can be obtained over 5 min without any discomfort or pain to the patient. Although there were some lesions that were not depicted because of their location outside the field of view, lesions were depicted with greater detail when they were within the scanning range, yielding reasonably high sensitivity.

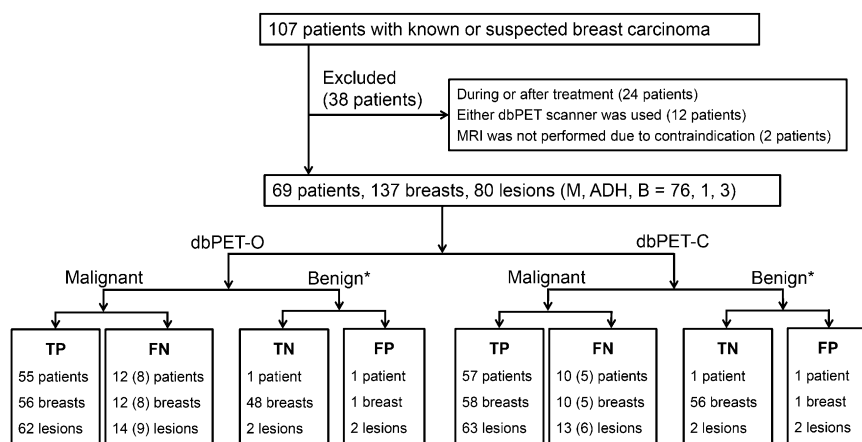


FIGURE 2. Flowchart demonstrates number of patients, breasts, and lesions evaluated with O and C scanners and their outcomes. Number in parentheses corresponds to patients, breasts, or lesions for which false-negative results were caused by tissue being outside field of view in dedicated PET. Total numbers of evaluated breasts are different between O PET ($n = 117$) and C PET ($n = 125$) because scanning was omitted for some breasts without suspected lesions. ADH = atypical ductal hyperplasia; B = benign; dbPET = dedicated breast PET; FN = false-negative; FP = false-positive; M = malignant; TN = true-negative; TP = true-positive. *Benign category includes 1 case of ADH.

TABLE 2
Number of Evaluated Lesions According to Histopathologic Findings

Finding	O PET (n = 80)	C PET (n = 80)
Malignant lesions	76 (95%)	76 (95%)
Invasive ductal carcinoma	67	67
Grade I	15 (13 within FOV)	15 (14 within FOV)
Grade II	41 (37 within FOV)	41 (38 within FOV)
Grade III	11 (9 within FOV)	11 (10 within FOV)
Invasive lobular carcinoma	5	5
Noninvasive carcinoma (DCIS)	4 (3 within FOV)	4 (3 within FOV)
Atypical ductal hyperplasia	1 (1%)	1 (1%)
Benign lesions	3 (4%)	3 (4%)
Fibroadenoma	1	1
Fibrocystic change	2	2

FOV = field of view.

In this study, excluding lesions outside the field of view, the patient-based and lesion-based sensitivities of O PET were 93% and 93%, respectively, and those of C PET were 92% and 90%, respectively, whereas those of PET/CT were 96% and 92%, respectively. It has been reported that the overall sensitivity of conventional ^{18}F -FDG PET for detecting breast cancer was 48%–95.7% (6) and that of other PEM system was approximately 90% (16). Despite the higher spatial resolution of our dedicated PET scanners, the overall sensitivity was almost comparable, after lesions outside the field of view were excluded, and rather lower than that of our conventional PET/CT and most of the sensitivities of whole-body PET/CT reported in the literature (23,28). Indeed there were some cases in which large and small lesions were separately identified on dedicated PET, whereas only 1 focus of intense uptake was observed on PET/CT, as is shown in Figure 3; however, some lesions close to the edge of the dedicated PET scanning range were not clearly depicted because of the noise, resulting in false-negative results. In addition, because patients for whom breast cancer was suspected were recruited in this study, relatively larger tumors (with an average size of 26 mm), large enough to be identified by a conventional PET/CT scanner, were assessed. Further prospective studies with a greater number of small tumors

would be necessary to evaluate the clinical efficacy of these dedicated PET scanners.

Nine lesions with the O scanner and 6 lesions with the C scanner were outside the field of view, despite efforts to manage this problem by patient positioning. All of the lesions that could not be imaged were close to the chest wall, consistent with the previous findings that the posterior portion of the breast might not be successfully imaged with PEM (12). This limited field of view is a limitation of these scanners, especially in Asian women with relatively smaller breasts. With the O scanner, the smaller gantry, with a 360° range of detectors, enabled a clear depiction of small lesions, but more lesions were outside the scanning range because of its smaller field of view. Conversely, with the C scanner, the field of view was larger than that of the O scanner, allowing both slightly more primary lesions and even nodal metastasis in the axilla to be detected, but some lesions were not as clearly visible because of increased noise caused by the C-shaped range detectors of the scanner.

The breast-based specificities of the O and C scanners were 98% and 98%, respectively, whereas that of PET/CT or MRI was 100%. Two fibrocystic change lesions identified on dedicated PET were not apparent on a PET/CT. Because ^{18}F -FDG accumulates in inflammatory foci, the higher sensitivity of dedicated PET may detect tiny foci

TABLE 3
Patient-Based Sensitivity and Specificity of Each Modality

Parameter	O PET	C PET	PET/CT	MRI
Sensitivity*	82% (55/67)	85% (57/67)	96% (64/67)	100% (67/67)
Sensitivity†	93% (55/59)	92% (57/62)	—	—
Specificity	50% (1/2)	50% (1/2)	100% (2/2)	50% (1/2)

*Sensitivity was calculated including patients with lesions outside field of view in dedicated PET.

†Sensitivity was calculated excluding patients with lesions outside field of view in dedicated PET.

TABLE 4
Breast-Based Sensitivity and Specificity of Each Modality

Parameter	O PET	C PET	PET/CT	MRI
Sensitivity*	82% (56/68)	85% (58/68)	96% (65/68)	100% (68/68)
Sensitivity†	93% (56/60)	92% (58/63)	—	—
Specificity	98% (48/49)	98% (56/57)	100% (70/70)	100% (70/70)

*Sensitivity was calculated including patients with lesions outside field of view in dedicated PET.

†Sensitivity was calculated excluding patients with lesions outside field of view in dedicated PET.

of hypermetabolism, causing false-positive findings. Therefore, it should be kept in mind that positive findings on dedicated PET do not always imply malignant breast tumors when ^{18}F -FDG is used as a radiotracer, and histopathologic confirmation is necessary before surgery. In this population, there were no new lesions identified unexpectedly on the contralateral side.

In the 2 cases for which we performed the immunohistochemical evaluation because the uptake pattern had been different between conventional PET/CT and dedicated PET, viable tumors with high hexokinase II activity were predominant in the peripheral portion within the tumor, which was consistent with the ringlike uptake on dedicated PET, although PET/CT had demonstrated almost homogeneous uptake (Fig. 4). There are some reports describing a centrally necrotizing tumor that often shows distinctive histologic features with a basallike immunophenotype and an aggressive and rapidly progressive course (29,30). It is expected that the finding of a ringlike uptake on dedicated PET may contribute to a prediction of patients' prognosis, but further evaluation with more patients and a longer follow-up is required to address this issue.

PET uptake is often used as a measure of semiquantitative ^{18}F -FDG uptake for PEM (31). However, in this investigation, dedicated PET images were not analyzed quantitatively because they were reconstructed without attenuation correction in our current system. Attenuation correction would have less effect in breast PET, when compared with PET of other organs, because the breast is small and homogeneous, composed essentially of fat tissue. Nevertheless, we are currently developing a software-based

attenuation correction scheme by detecting the contour of the breast.

As previously mentioned, some lesions were outside the field of view in our study, which is a limitation. In the depiction of posterior lesions, breast MRI excels. However, when lesions are within the field of view, the higher spatial resolution of dedicated PET, as compared with conventional PET/CT, can reveal tumors with more precise functional and morphologic information. Dedicated PET might yield more accurate information for monitoring therapy response to chemotherapy if ^{18}F -FDG is used as the tracer. In addition, if more specific tracers target tissue or other tumor components, the higher spatial resolution and sensitivity of these scanners would be helpful for evaluating lesions. Therefore, the development of new probes specific for breast imaging is expected, although guidance for lesion biopsy might be difficult with this system.

This study has some other limitations. First, we analyzed just 2 lesions per 1 breast for 4 patients with multifocal lesions. Biopsy is usually performed for 2 lesions but is sometimes omitted for other lesions because the therapeutic strategy is not changed. Also, neoadjuvant chemotherapy is often conducted before surgery, and it is difficult to get an accurate comparison between radiologic findings and histopathologic results for small lesions that had not been examined by biopsy. To avoid unreliable correlations, we limited the maximum number of assessed lesions per breast to 2, possibly resulting in an overestimation of the sensitivity of dedicated PET. In this investigation, 54 lesions were examined by biopsy before PET. Lesion visibility, however, was not affected by whether biopsy was performed, probably because there was a relatively

TABLE 5
Lesion-Based Sensitivity and Specificity of Each Modality

Parameter	O PET	C PET	PET/CT	MRI
Sensitivity*	82% (62/76)	83% (63/76)	92% (70/76)	100% (76/76)
Sensitivity†	93% (62/67)	90% (63/70)	—	—
Specificity	50% (2/4)	50% (2/4)	100% (4/4)	75% (3/4)

*Sensitivity was calculated including patients with lesions outside field of view in dedicated PET.

†Sensitivity was calculated excluding patients with lesions outside field of view in dedicated PET.

TABLE 6
Sensitivities According to T Stage and Histopathologic Results

Result	O PET	C PET	PET/CT
T staging			
T1a	50% (1/2)	50% (1/2)	0% (0/2)
T1b	67% (4/6)	67% (4/6)	71% (5/7)
T1c	96% (22/23)	92% (23/25)	96% (26/27)
T2	96% (24/25)	96% (25/26)	96% (27/28)
T3	100% (8/8)	100% (8/8)	100% (8/8)
Histopathology			
Invasive ductal carcinoma	93% (55/59)	94% (58/62)	93% (62/67)
Grade I	85% (11/13)	86% (12/14)	94% (14/15)
Grade II	95% (35/37)	95% (36/38)	91% (37/41)
Grade III	100% (9/9)	100% (10/10)	100% (11/11)
Invasive lobular carcinoma	80% (4/5)	60% (3/5)	80% (4/5)
DCIS	100% (3/3)	67% (2/3)	100% (4/4)

Nine lesions were outside field of view in O PET and 6 lesions in C PET. These lesions were excluded from analysis.

large tumor in many instances. However, if a greater number of small tumors are to be evaluated, the sensitivity may be influenced by the procedure. In addition, WB PET/CT was performed at approximately 60 min, whereas the average uptake phase was more than 100 min in dedicated PET. Because it is known that the radioactive uptake of a malignant lesion can continue to increase after injection in many cases (32), a longer uptake phase could also result in an overestimation of the sensitivity of dedicated PET.

CONCLUSION

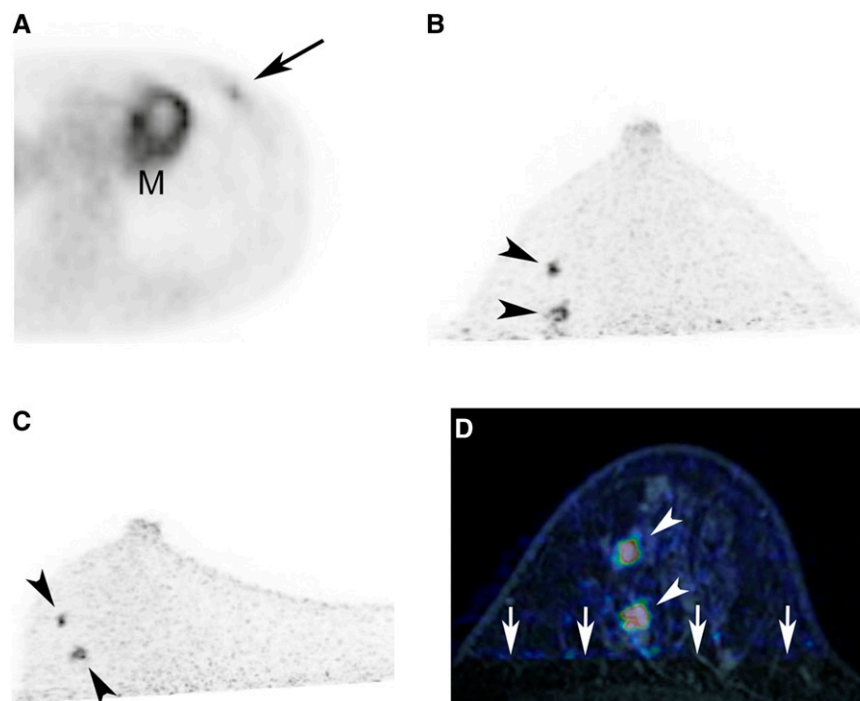
Two kinds of newly developed dedicated PET scanner both are clinically feasible and had reasonably high

sensitivity in patients with breast cancer. Because some lesions close to the chest wall were outside the field of view, overall sensitivity was lower than that of conventional whole-body PET/CT, but more precise histopathologic information was provided by these dedicated scanners. Further evaluations with more patients are needed to assess the diagnostic performance of these scanners for nonpalpable lesions, including DCIS, and to investigate the prognostic value of the dedicated PET images.

DISCLOSURE STATEMENT

The costs of publication of this article were defrayed in part by the payment of page charges. Therefore, and solely

FIGURE 3. Invasive ductal carcinoma of left breast in 41-y-old woman. Only 1 focus of moderate uptake is observed on PET portion of conventional PET/CT (A; arrow), whereas 2 foci of intense uptake can be seen on O PET (B; arrowheads) and C PET (C, arrowheads). Scanning position was different between conventional PET/CT and dedicated PET—that is, supine vs. prone or forward-leaning. On fused image of dedicated PET and contrast-enhanced MRI, 2 cases of focal uptake correspond to enhanced nodules (D; arrowheads), suggesting breast cancers, which were confirmed by surgery. Posterior breast tissues are not fully included because of limited field of view of dedicated PET, compared with MRI (D; arrows). M = indicates physiologic uptake in myocardium.



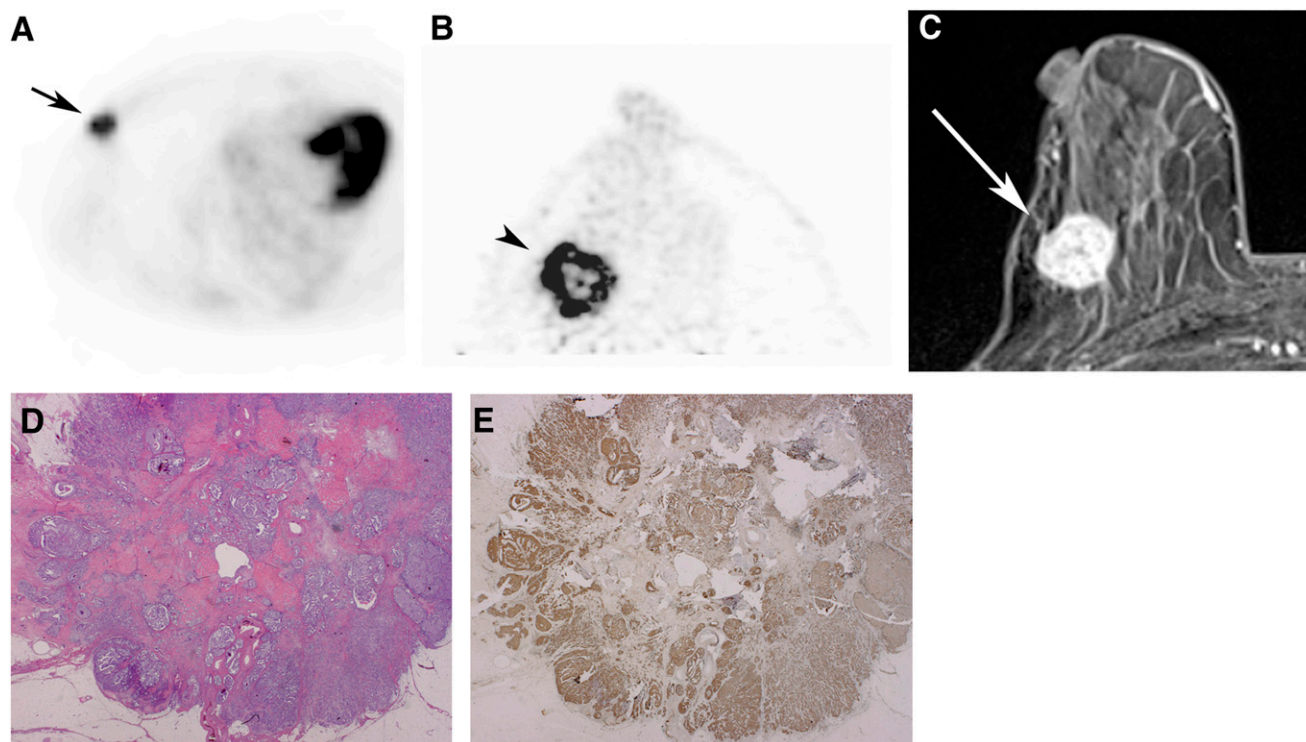


FIGURE 4. Invasive ductal carcinoma of right breast in 77-y-old woman. Conventional PET/CT reveals focal intense uptake (A; arrow), whereas ringlike uptake is observed on O PET (B; arrowhead), corresponding to enhanced lesion on MRI (C; arrow). With histopathologic examination, central necrosis is evident in hematoxylin and eosin staining (D). In addition, hexokinase II activity (E) is predominant mainly in peripheral area within tumor, which is consistent with finding by dedicated PET.

to indicate this fact, this article is hereby marked “advertisement” in accordance with 18 USC section 1734.

ACKNOWLEDGMENTS

We thank Tae Oishi, RT/CNMT, for her excellent clinical assistance; Masafumi Furuta, Junichi Ohi, and Keishi Kitamura for their technical advice; and Dr. Denis Le Bihan for his kind suggestions. We obtained financial support from Shimadzu Corporation, Kyoto, Japan, and a Grant-in-Aid for Scientific Research from the Ministry of Education, Culture, Sports, Science and Technology of Japan (C:22591329). No other potential conflict of interest relevant to this article was reported.

REFERENCES

1. Siegel R, Ward E, Brawley O, Jemal A. Cancer statistics, 2011. *CA Cancer J Clin*. 2011;61:212–236.
2. Tabár L, Vitak B, Chen HHT, Yen MF, Duffy SW, Smith RA. Beyond randomized controlled trials. *Cancer*. 2001;91:1724–1731.
3. Wahl R, Cody R, Hutchins G, Mudgett E. Primary and metastatic breast carcinoma: initial clinical evaluation with PET with the radiolabeled glucose analogue 2-[F-18]-fluoro-2-deoxy-D-glucose. *Radiology*. 1991;179:765–770.
4. Adler L, Crowe J, Al-Kaisi N, Sunshine J. Evaluation of breast masses and axillary lymph nodes with [F-18] 2-deoxy-2-fluoro-D-glucose PET. *Radiology*. 1993;187:743–750.
5. Avril N, Dose J, Janicke F, et al. Metabolic characterization of breast tumors with positron emission tomography using F-18 fluorodeoxyglucose. *J Clin Oncol*. 1996;14:1848–1857.
6. Escalona S, Blasco J, Reza M, Andradas E, Gomez N. A systematic review of FDG-PET in breast cancer. *Med Oncol*. 2010;27:114–129.
7. Scheidhauer K, Walter C, Seemann M. FDG PET and other imaging modalities in the primary diagnosis of suspicious breast lesions. *Eur J Nucl Med Mol Imaging*. 2004;31:S70–79.
8. Levine EA, Freimanis RI, Perrier ND, et al. Positron emission mammography: initial clinical results. *Ann Surg Oncol*. 2003;10:86–91.
9. Freifelder R, Karp JS. Dedicated PET scanners for breast imaging. *Phys Med Biol*. 1997;42:2463–2480.
10. Raylman RR, Majewski S, Smith MF, et al. Comparison of scintillators for positron emission mammography (PEM) systems. *IEEE Trans Nucl Sci*. 2003;50:42–49.
11. Bowen SL, Wu Y, Chaudhari AJ, et al. Initial characterization of a dedicated breast PET/CT scanner during human imaging. *J Nucl Med*. 2009;50:1401–1408.
12. Rosen EL, Turkington TG, Soo MS, Baker JA, Coleman RE. Detection of primary breast carcinoma with a dedicated, large-field-of-view FDG PET mammography device: initial experience. *Radiology*. 2005;234:527–534.
13. MacDonald L, Edwards J, Lewellen T, Haseley D, Rogers J, Kinahan P. Clinical imaging characteristics of the positron emission mammography camera: PEM Flex Solo II. *J Nucl Med*. 2009;50:1666–1675.
14. Raylman RR, Majewski S, Smith MF, et al. The positron emission mammography/tomography breast imaging and biopsy system (PEM/PET): design, construction and phantom-based measurements. *Phys Med Biol*. 2008;53:637–653.
15. Tai YC, Wu H, Pal D, O’Sullivan JA. Virtual-pinhole PET. *J Nucl Med*. 2008;49:471–479.
16. Berg WA, Weinberg IN, Narayanan D, et al. High-resolution fluorodeoxyglucose positron emission tomography with compression (“positron emission mammography”) is highly accurate in depicting primary breast cancer. *Breast J*. 2006;12:309–323.
17. Berg WA, Madsen KS, Schilling K, et al. Breast cancer: comparative effectiveness of positron emission mammography and MR imaging in presurgical planning for the ipsilateral breast. *Radiology*. 2011;258:59–72.
18. Schilling K, Narayanan D, Kalinyak JE, et al. Positron emission mammography in breast cancer presurgical planning: comparisons with magnetic resonance imaging. *Eur J Nucl Med Mol Imaging*. 2011;38:23–36.

19. Nakamoto Y, Ishizu K, Kanao S, Kawai K, Togashi K. Clinical imaging characteristics of the newly developed PET scanner for breast imaging [abstract]. *J Nucl Med*. 2010;51(suppl 2):220P.
20. Furuta M, Kitamura K, Ohi J, et al. Basic evaluation of a C-shaped breast PET scanner. *Proc IEEE Nuc Sci Symp Conf Rec*. 2009;2548–2552.
21. Nakayama T, Kudo H. Derivation and implementation of ordered-subsets algorithms for list-mode PET data. *Proc IEEE Nuc Sci Symp Conf Rec*. 2005;5.
22. Ikeda DM, Hylton NM, Kuhl CK, et al. *Breast Imaging Reporting and Data System, BI-RADS: Magnetic Resonance Imaging*. Reston, VA: American College of Radiology; 2003.
23. Avril N, Rose C, Schelling M, et al. Breast imaging with positron emission tomography and fluorine-18 fluorodeoxyglucose: use and limitations. *J Clin Oncol*. 2000;18:3495–3502.
24. Eby PR, DeMartini WB, Gutierrez RL, Saini MH, Peacock S, Lehman CD. Characteristics of probably benign breast MRI lesions. *AJR*. 2009;193:861–867.
25. Tavassoli FA, Devilee P. *World Health Organization Classification of Tumours: Pathology and Genetics of Tumours of the Breast and Female Genital Organs*. Lyon, France: IARC Press; 2003.
26. Thompson C, Murthy K, Weinberg I, Mako F. Feasibility study for positron emission mammography. *Med Phys*. 1994;21:529–538.
27. Tafra L, Cheng Z, Uddo J, et al. Pilot clinical trial of ¹⁸F-fluorodeoxyglucose positron-emission mammography in the surgical management of breast cancer. *Am J Surg*. 2005;190:628–632.
28. Heusner TA, Kuemmel S, Umutlu L, et al. Breast cancer staging in a single session: whole-body PET/CT mammography. *J Nucl Med*. 2008;49:1215–1222.
29. Yu L, Yang W, Cai X, Shi D, Fan Y, Lu H. Centrally necrotizing carcinoma of the breast: clinicopathological analysis of 33 cases indicating its basal-like phenotype and poor prognosis. *Histopathology*. 2010;57:193–201.
30. Jimenez RE, Wallis T, Visscher DW. Centrally necrotizing carcinomas of the breast: a distinct histologic subtype with aggressive clinical behavior. *Am J Surg Pathol*. 2001;25:331–337.
31. Narayanan D, Madsen KS, Kalinyak JE, Berg WA. Interpretation of positron emission mammography: feature analysis and rates of malignancy. *AJR*. 2011;196:956–970.
32. Basu S, Alavi A. Partial volume correction of standardized uptake values and the dual time point in FDG-PET imaging: should these be routinely employed in assessing patients with cancer? *Eur J Nucl Med Mol Imaging*. 2007;34:1527–1529.



The Journal of
NUCLEAR MEDICINE

Clinical Performance of 2 Dedicated PET Scanners for Breast Imaging: Initial Evaluation

Mami Iima, Yuji Nakamoto, Shotaro Kanao, Tomoharu Sugie, Takayuki Ueno, Mayumi Kawada, Yoshiki Mikami, Masakazu Toi and Kaori Togashi

J Nucl Med. 2012;53:1534-1542.

Published online: August 29, 2012.

Doi: 10.2967/jnumed.111.100958

This article and updated information are available at:

<http://jnm.snmjournals.org/content/53/10/1534>

Information about reproducing figures, tables, or other portions of this article can be found online at:

<http://jnm.snmjournals.org/site/misc/permission.xhtml>

Information about subscriptions to JNM can be found at:

<http://jnm.snmjournals.org/site/subscriptions/online.xhtml>

The Journal of Nuclear Medicine is published monthly.
SNMMI | Society of Nuclear Medicine and Molecular Imaging
1850 Samuel Morse Drive, Reston, VA 20190.
(Print ISSN: 0161-5505, Online ISSN: 2159-662X)

© Copyright 2012 SNMMI; all rights reserved.

The logo for the Society of Nuclear Medicine and Molecular Imaging (SNMMI) consists of the letters 'S', 'N', 'M', and 'I' arranged in a 2x2 grid. Each letter is white and set within a red square. To the right of this grid, the full name of the society is written in a sans-serif font.
SOCIETY OF
NUCLEAR MEDICINE
AND MOLECULAR IMAGING